



Gene Expression Profiles of Human Cerebral Organoids Identify PPAR Pathway and *PKM2* as Key Markers for Oxygen-Glucose Deprivation and Reoxygenation

OPEN ACCESS

Edited by:

Li Li,
Capital Medical University, China

Reviewed by:

Zhisong He,
ETH Zurich, Switzerland
Silvia Bolognin,
University of
Luxembourg, Luxembourg

*Correspondence:

Eiichiro Mori
emori@naramed-u.ac.jp
Kazuma Sugie
ksugie@naramed-u.ac.jp

†These authors have contributed
equally to this work

Specialty section:

This article was submitted to
Cellular Neuropathology,
a section of the journal
Frontiers in Cellular Neuroscience

Received: 11 September 2020

Accepted: 10 May 2021

Published: 08 June 2021

Citation:

Iwasa N, Matsui TK, Iguchi N,
Kinugawa K, Morikawa N,
Sakaguchi YM, Shiota T,
Kobashigawa S, Nakanishi M,
Matsubayashi M, Nagata R, Kikuchi S,
Tanaka T, Eura N, Kiriyama T, Izumi T,
Saito K, Kataoka H, Saito Y, Kimura W,
Wanaka A, Nishimura Y, Mori E and
Sugie K (2021) Gene Expression
Profiles of Human Cerebral Organoids
Identify PPAR Pathway and *PKM2* as
Key Markers for Oxygen-Glucose
Deprivation and Reoxygenation.
Front. Cell. Neurosci. 15:605030.
doi: 10.3389/fncel.2021.605030

Naoki Iwasa^{1†}, Takeshi K. Matsui^{1,2†}, Naohiko Iguchi¹, Kaoru Kinugawa¹,
Naritaka Morikawa², Yoshihiko M. Sakaguchi², Tomo Shiota¹, Shinko Kobashigawa²,
Mari Nakanishi², Masaya Matsubayashi², Riko Nagata², Sotaro Kikuchi²,
Tatsuhide Tanaka³, Nobuyuki Eura¹, Takao Kiriyama¹, Tesseki Izumi¹, Kozue Saito¹,
Hiroshi Kataoka¹, Yuichi Saito⁴, Wataru Kimura⁴, Akio Wanaka³, Yuhei Nishimura⁵,
Eiichiro Mori^{2,6*} and Kazuma Sugie^{1*}

¹ Department of Neurology, Nara Medical University, Kashihara, Japan, ² Department of Future Basic Medicine, Nara Medical University, Kashihara, Japan, ³ Department of Anatomy and Neuroscience, Nara Medical University, Kashihara, Japan, ⁴ Laboratory for Heart Regeneration, RIKEN Center for Biosystems Dynamics Research, Kobe, Japan, ⁵ Department of Integrative Pharmacology, Mie University Graduate School of Medicine, Tsu, Japan, ⁶ V-iCliniX Laboratory, Nara Medical University, Kashihara, Japan

Ischemic stroke is one of the most common neurological diseases. However, the impact of ischemic stroke on human cerebral tissue remains largely unknown due to a lack of ischemic human brain samples. In this study, we applied cerebral organoids derived from human induced pluripotent stem cells to evaluate the effect of oxygen-glucose deprivation/reoxygenation (OGD/R). Pathway analysis showed the relationships between vitamin digestion and absorption, fat digestion and absorption, peroxisome proliferator-activated receptor (PPAR) signaling pathway, and complement and coagulation cascades. Combinational verification with transcriptome and gene expression analysis of different cell types revealed fatty acids-related PPAR signaling pathway and pyruvate kinase isoform M2 (*PKM2*) as key markers of neuronal cells in response to OGD/R. These findings suggest that, although there remain some limitations to be improved, our ischemic stroke model using human cerebral organoids would be a potentially useful tool when combined with other conventional two-dimensional (2D) mono-culture systems.

Keywords: cerebral organoid, human induced pluripotent stem cells, oxygen-glucose deprivation/reoxygenation, ischemic stroke, pyruvate kinase M2, peroxisome proliferator-activated receptor, ferritin light chain

INTRODUCTION

Stroke, a cerebrovascular disease, is a common neurological disorder, and ischemic strokes are among the major causes of permanent morbidity and disability (Spescha et al., 2013; Knowland et al., 2014; Benjamin et al., 2019). Several therapeutic agents are available for acute ischemic stroke, including thrombolytics, anticoagulants, and antiplatelets. However, their efficacy is restricted and

their use is limited (Catanese et al., 2017). Mechanical thrombolytics and recombinant tissue plasminogen activator (rt-PA) have therapeutic time windows for hyperacute ischemic stroke, because the target of these therapies is to rescue the penumbra around the ischemic core (Fisher and Bastan, 2012; Dorado et al., 2014). Thus, elucidating the mechanism of ischemic stroke in human cerebral tissue is expected to be important for the development of appropriate therapies.

Thus far, two-dimensional (2D) neuron cultures have been utilized in ischemic models. However, there are limitations to these models as actual brain tissues are composed of multiple cell types and responses to ischemia take place from cell to cell. Recent progress in the development of organs in-a-dish (organoids) provides potential for the modeling of various diseases (Clevers, 2016). Organoids resemble the architecture of organs that are composed of multiple cell types, and three-dimensionally (3D) cultured cerebral organoids are expected to represent physiological environment (Pasca et al., 2015). In this study, we analyzed the gene expression profiles of human cerebral organoids after oxygen-glucose deprivation/reoxygenation (OGD/R).

MATERIALS AND METHODS

Human Cerebral Organoids Generation and Culture

Human induced pluripotent stem cells (iPSCs) which were Cellartis Human iPS Cell Line 12 (ChiPSC12, Y00285, Takara Bio, Kusatsu, Shiga, Japan) were cultivated in mTeSR-TM1 medium (05851, Stemcell Technologies, Vancouver, British Columbia, Canada) and maintained in feeder-free condition with mTeSR-TM1 media. Feeder-free human iPSC line (XY) from Takara was obtained on six well plates (3506, Corning, New York, USA) coated with growth factors reduced Matrigel (356230; BD Biosciences, San Jose, CA, USA). At the time of passage, we added Rho-associated protein kinase (ROCK) inhibitor (final concentration 10 μ M; Selleck Chemicals, Houston, Texas, USA), and maintained these cells with daily medium change without ROCK inhibitor until they reached about 70% confluency. Then, they were detached by versene solution (15040-066; Thermo Fisher Scientific, Waltham, MA, USA) and seeded by a 1:20 dilution ratio.

Cerebral organoids were differentiated according to previously published protocol (Lancaster et al., 2013). Human iPSCs were detached and subjected to embryoid body (EB) induction using the protocol. After 4 days, half of the media was replaced by human EB medium without ROCK inhibitor and basic fibroblast growth factor (bFGF). Two days later, the EBs were transferred into a neural induction media which consisted of DMEM-F12 with 1 \times N2 supplement (17502048; Thermo Fisher Scientific, Waltham, MA, USA), 1 \times GlutaMax, 1 \times non-essential amino acids, and heparin (1 μ g/ml) and then embedded in Matrigel after 5 days. Subsequently, the organoids were induced in organoid medium by using an orbital shaker. The total process took 6 weeks, from EB formation.

Immunohistochemical Analysis of Human Cerebral Organoids

Human cerebral organoids were fixed in 4% paraformaldehyde in Phosphate-Buffered Saline (PBS) overnight at 4°C, dehydrated with 30% sucrose in PBS and embedded in O.C.T. Compound (Thermo Fisher Scientific, Waltham, MA, USA). Cryostat sections (14 μ m) were cut and mounted on slides (Thermo Fisher Scientific, Waltham, MA, USA). Mounted sections were incubated at room temperature for 1 h with blocking solution [3% normal goat serum + 0.3% Triton X-100 in tris-buffered saline (TBS)] and subsequently incubated with primary antibodies diluted in blocking solution overnight at 4°C. Antibodies specific for TUJ1 (1:400, T8660, Sigma-Aldrich, St. Louis, Missouri, USA) were used for immunostaining. After three washes with TBS, corresponding fluorescent dye Alexa Fluor 488-conjugated anti-mouse IgG (715-545-151, Jackson ImmunoResearch, West Grove, PA, USA) secondary antibodies diluted in the blocking solution were added and samples were incubated at room temperature for 2 h and followed by 4',6-diamidino-2-phenylindole (DAPI) (Vectashield Mounting Medium with DAPI, H-200; Vector Laboratories, Burlingame, CA, USA) staining. Finally, stained slides were rinsed with TBS three times, mounted, and analyzed using a FV3000 Confocal Microscope (Olympus, Shinjuku, Tokyo, Japan).

Oxygen-Glucose Deprivation/Reoxygenation and RNA Extraction of Human Cerebral Organoids

The organoids were plated in Dulbecco's Modified Eagle Medium without glucose [DMEM (No Glucose), 09891-25; NACALAI TESQUE, Kyoto, Kyoto, Japan], and 1% penicillin-streptomycin (26253-84; NACALAI TESQUE, Kyoto, Kyoto, Japan). Subsequently, the organoids were cultured in a hypoxic incubator (94% N₂, 5% CO₂, 1% O₂) at 37°C for 1 h. For reoxygenation, the medium was changed to Primary Neuron Basal Medium, then incubated (95% air, 5% CO₂) at 37°C for 1 h. RNA from human cerebral organoids was extracted according to the manufacturer's protocol supplied with TRIzol reagent (15596018; Thermo Fisher Scientific, Waltham, MA, USA). The concentration and purity of the RNA samples were measured using Spectrophotometer (Beckman Coulter, Brea, California, USA).

RNA Sequencing of Human Cerebral Organoids

Total RNA was isolated from the cells using the PureLink RNA Mini Kit (12183020; Thermo Fisher Scientific, Waltham, MA, USA) and according to the manufacturer's instructions. RNA concentration was analyzed by Qubit RNA HS Assay Kit (Thermo Fisher Scientific, Waltham, MA, USA) and the purity was assessed using the Qsep100 DNA Fragment Analyzer and RNA R1 Cartridge (BioOptic, New Taipei City, Taiwan). For RNA-sequencing (RNA-seq) analysis, each extracted RNA sample of non-treated organoid in equal concentration was adopted, and the same was adopted for OGD/R. Extracted RNA samples were either sent to a Bioengineering lab for RNA-sequencing analysis,

and or subjected to RT-PCR. Then, total RNA was converted to cDNA and used for Illumina sequencing library preparation, according to KAPA Stranded mRNA-Seq Kit protocols (KAPA Biosystems, Wilmington, MA, United States). DNA fragments were ligated by FastGene Adapter Kit (NIPPON Genetics, Bunkyo, Tokyo, Japan). After the purified cDNA library products were appreciated using Qubit dsDNA HS Assay Kit (Thermo Fisher Scientific, Waltham, MA, USA), they were qualitatively evaluated using the Fragment Analyzer and dsDNA 915 Reagent Kit (Advanced Analytical Technologies) before it was finally sequenced (2×76 bp) on NextSeq 500 (Illumina, San Diego, CA, United States). Sickle (ver.1.33) is an error correction tool for quality trimming. It discards reads based upon the length threshold derived from quality score for FASTQ files. Using Sickle (ver.1.33), the threshold identified were quality values under 20 base and reads under 30 bp. Additionally, Hisat2 software was run with default parameters. The sequence alignment files generated by Sickle and Hisat2 were used to generate counts of mapped reads.

Differentially Expressed Genes Extraction of Human Cerebral Organoids

By comparing organoids under OGD/R condition to non-treated organoids and using R package edgeR (Robinson et al., 2010) in R software (version 3.5.3), differentially expressed genes (DEGs) were extracted. The MA plot in R is a visual tool for showing the total gene expression levels of DEGs. The X-axis represents $\log \text{CPM} - \log$ counts per million—and are measures of gene expression level. The Y-axis indicates $\log \text{FC}$. $\log \text{FC}$ is the \log fold-change, which in this case, is the \log difference between cerebral organoids after OGD/R.

Gene Ontology and Pathway Analysis of Human Cerebral Organoids

Using the Database for Annotation, Visualization, and Integrated Discovery [DAVID, version 6.8 database (<https://david.ncifcrf.gov/>)], selected DEGs were analyzed. The DAVID shows the molecular function, biological process, and cellular component expressed in the gene profile. In this study, DAVID was applied to evaluate gene ontological (GO) annotation and Kyoto encyclopedia of genes and genomes (KEGG) pathways of DEGs. P -value < 0.05 was chosen as the threshold of KEGG pathway. Upregulation and downregulation of genes were analyzed separately.

Protein–Protein Interaction Analysis of Human Cerebral Organoids

Based on the Search Tool for the Retrieval of Interacting Genes (STRING, <https://string-db.org/>; Szklarczyk et al., 2019) online database, DEGs were inputted, and the protein–protein interaction (PPI) network was constructed. The STRING database shows the interaction of each protein from prediction or experiments. The threshold to construct the PPI network was confidence score > 0.4 .

Reverse Transcriptase-Polymerase Chain Reaction and Quantitative Polymerase Chain Reaction of Human Cerebral Organoids

For RT-PCR, the extracted RNAs were reverse transcribed using the protocol supplied with ReverTra Ace qPCR RT Master Mix (FSQ-201; TOYOBO, Osaka, Osaka, Japan). StepOne Plus Real-time PCR System (Thermo Fisher Scientific, Waltham, MA, USA) was used to amplify and quantify levels of target gene cDNA. Quantitative PCR (q-PCR) was conducted using SsoAdvanced Universal SYBR Green Supermix (172-5271; BioRad Laboratories, Hercules, CA, United States) and specific primers for q-PCR. Primers used in this study are listed in **Supplementary Table 1**. Reactions were run in triplicate. The expression of each gene was normalized to the geometric mean of β -actin (10025636; BioRad Laboratories, Hercules, CA, United States) as a housekeeping gene and analyzed using the $\Delta\Delta\text{CT}$ method. Statistical analysis was performed using the GraphPad Prism7 (GraphPad Software). A two-tailed unpaired Student's t -test was applied to the q-PCR data. P -value < 0.05 was defined as the threshold.

Tissue-Specific Gene Expression Analysis

Gene expression data for normal human tissues were analyzed from the genotype tissue expression project (GTEx) portal (<http://www.gtexportal.org/home/>) to compare the similarity of expression pattern of some genes.

Oxygen-Glucose Deprivation/Reoxygenation of Human Hepatocellular Carcinoma and Quantitative Polymerase Chain Reaction

The HepG2 which were human hepatocellular carcinoma cell line (Cellular Engineering Technologies, Inc., Coralville, IA, USA) were maintained in growth medium (RPMI1640; NACALAI TESQUE, Kyoto, Kyoto, Japan) supplemented with 10% fetal bovine serum (HyClone, SH30396.03, GE Healthcare Life Sciences, Logan, UT, USA), 1% penicillin-streptomycin (26253-84; NACALAI TESQUE, Kyoto, Kyoto, Japan). The cells were incubated at 37°C in 5% CO_2 . Subsequently, cultured HepG2 cells were plated in DMEM without glucose (09891-25; NACALAI TESQUE, Kyoto, Kyoto, Japan), and 1% penicillin-streptomycin (26253-84; NACALAI TESQUE, Kyoto, Kyoto, Japan). Subsequently, the organoids were cultured in a hypoxic incubator (94% N_2 , 5% CO_2 , 1% O_2) at 37°C for 1 h. For reoxygenation, the medium was changed to growth medium, then incubated (95% air, 5% CO_2) at 37°C for 1 h. After cell culture, RNA extraction, RT-PCR and q-PCR were performed using the same procedure of human cerebral organoids. The sequences of primers used in this study are listed in **Supplementary Table 1**.

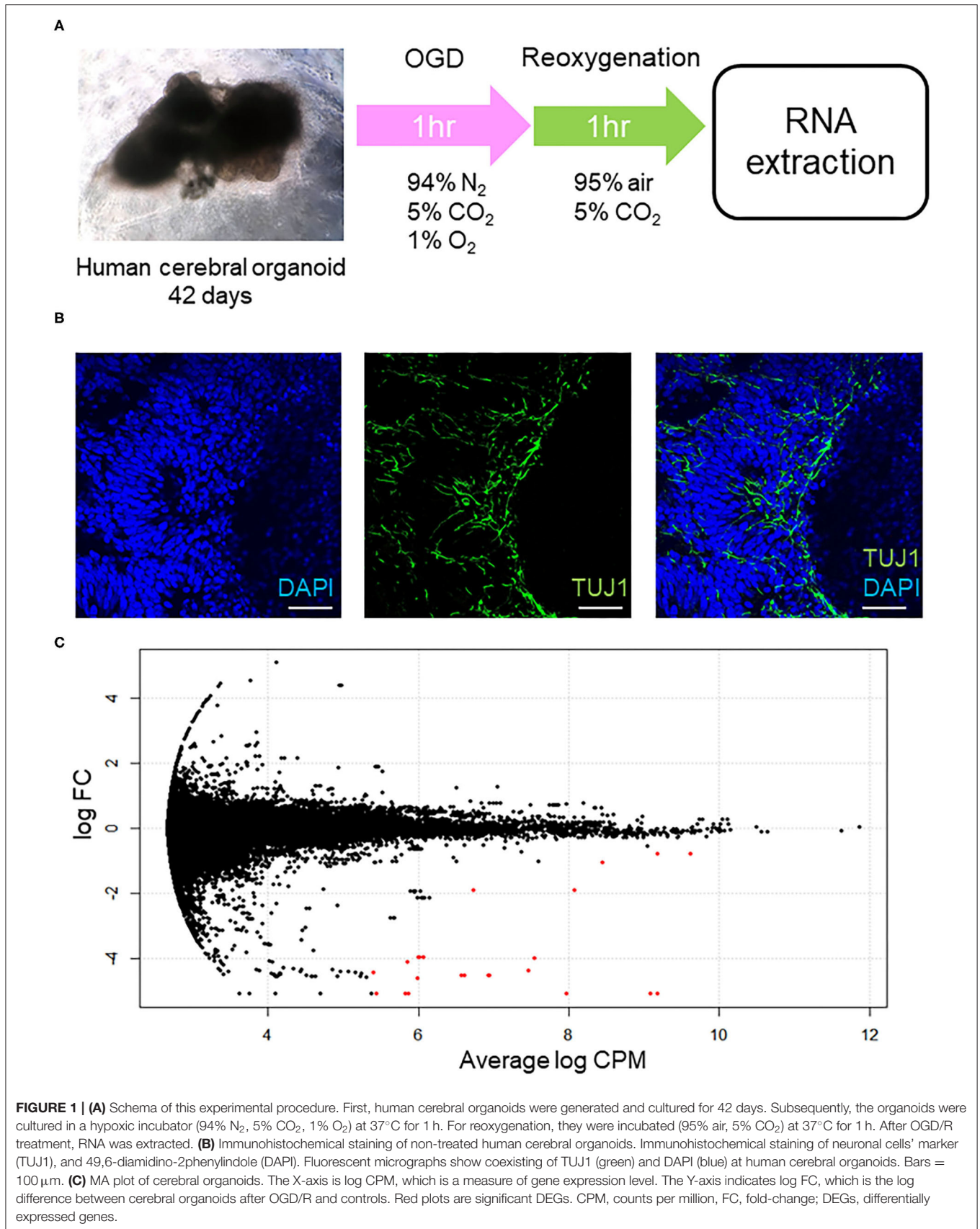


TABLE 1 | Profiling gene expression comparing organoids under OGD/R condition with non-treated organoids.

Gene symbol	logFC	P-value	FDR	Stage
AFP	-5.05202426	6.61E-89	1.19E-83	Down
TTR	-4.829589384	1.19E-37	7.09E-33	Down
APOA2	-4.375589058	1.38E-24	6.18E-20	Down
ALB	-3.992565039	4.23E-24	1.52E-19	Down
APOA1	-4.544446565	1.37E-17	3.52E-13	Down
RNA28SN4	-1.909649871	2.98E-14	5.94E-10	Down
APOC3	-4.616288539	1.08E-09	1.76E-05	Down
FTL	-0.803043639	2.06E-09	3.08E-05	Down
AHSG	-3.975861808	5.40E-09	7.45E-05	Down
FGG	-4.858272075	7.92E-09	0.0001015	Down
FABP1	-4.10691844	1.31E-07	0.00123622	Down
MIR3615	-1.070468786	1.86E-07	0.00167334	Down
FGB	-4.756570983	2.98E-06	0.02353793	Down
RNA45SN4	-1.899507421	3.02E-06	0.02353793	Down
FGA	-4.451593603	5.72E-06	0.04279685	Down
TF	-4.591735052	2.10E-05	0.14485088	Down
RBP4	-4.460754954	4.01E-05	0.2567811	Down
APOE	-2.151241972	4.23E-05	0.26168457	Down
SELENOP	-2.776594398	4.92E-05	0.29458499	Down
RN7SL2	1.271175267	0.0001831	0.88837764	Down
MIR4709	-1.029200022	0.0002927	1	Down
APOB	-4.704983376	0.0004883	1	Down
GPC3	-1.985098838	0.0005083	1	Down
ALDH1A1	-4.546504241	0.0005188	1	Down
YWHAE	4.380630428	0.0005188	1	Up
PTN	0.775148705	0.0005895	1	Up
s-rRNA	-0.5481881	0.0007606	1	Down
PMEL	-4.567564523	0.0009766	1	Down
NNAT	0.610458501	0.0026105	1	Up
RN7SL1	1.232302556	0.0038383	1	Up
GSTA1	-4.403571625	0.0039063	1	Down
APOA4	-4.361854192	0.0039063	1	Down
POSTN	0.705402287	0.0051026	1	Up
SERPINA1	-3.780463098	0.0063477	1	Down
DNAJB1	1.887700371	0.0066108	1	Up
RNA18SN5	-2.370210664	0.0073853	1	Down
MIR6132	1.736743211	0.0146333	1	Up
LOC105379506	5.83933038	0.015625	1	Up
RBP2	-4.698155314	0.015625	1	Down
DCT	-4.574216819	0.015625	1	Down
AMBP	-3.45106874	0.0214844	1	Down
VTN	-3.157212671	0.0214844	1	Down
H19	-3.053228094	0.0214844	1	Down
PEA15	0.753258601	0.0238198	1	Up
TUBA1A	0.250293775	0.025046	1	Up
MIR1244-1	-0.274612882	0.0268679	1	Down
SPINK1	-4.120454121	0.03125	1	Down
RPS6	-0.293592327	0.0351882	1	Down
MIR4442	0.351338228	0.0366267	1	Up
HSPA8	0.404708278	0.0390529	1	Up
MIR9-2	0.832371451	0.039617	1	Up
TMSB10	0.247345492	0.0457451	1	Up

Oxygen-Glucose Deprivation/Reoxygenation of Fibroblast, Glioblastoma and Murine Microglia, and Quantitative Polymerase Chain Reaction

Human telomerase reverse transcriptase immortalized fibroblasts (hTERT-BJ), human glioblastoma cell line (U251MG; obtained from Japanese collection of research bioresources) and murine microglial cell line (BV2 cells) were cultured in DMEM with 4.5 g/l glucose (08459-64; NACALAI TESQUE, Kyoto, Kyoto, Japan) supplemented with 10% fetal bovine serum (HyClone, SH30396.03, GE Healthcare Life Sciences, Logan, UT, USA), 1% penicillin-streptomycin (26253-84; NACALAI TESQUE, Kyoto, Kyoto, Japan). The cells were incubated at 37°C in 5% CO₂. Subsequently, cultured hTERT-BJ, U251MG, and BV2 cells were maintained or plated in DMEM without glucose (09891-25; NACALAI TESQUE, Kyoto, Kyoto, Japan) supplemented with 10% fetal bovine serum (HyClone, SH30396.03, GE Healthcare Life Sciences, Logan, UT, USA), 1% penicillin-streptomycin (26253-84; NACALAI TESQUE, Kyoto, Kyoto, Japan). Hypoxic experiments were performed in a CBS-90 hypoxia workstation (ASTEC, Kasuya, Fukuoka, Japan) at 37°C under severe hypoxic (1% oxygen) or mild conditions (10% oxygen). hTERT-BJ, U251MG, and BV2 cells plated in DMEM with 4.5 g/l glucose (08459-64; NACALAI TESQUE, Kyoto, Kyoto, Japan) or DMEM without glucose (09891-2; NACALAI TESQUE, Kyoto, Kyoto, Japan) were cultured in a hypoxic incubator (94% N₂, 5% CO₂, 1% O₂) at 37°C for 1 h. The mild hypoxic condition we used was 10% oxygen for 24 h. For reoxygenation, the medium was changed to DMEM with 4.5 g/l glucose (08459-64; NACALAI TESQUE, Kyoto, Kyoto, Japan) supplemented with 10% fetal bovine serum (HyClone, SH30396.03, GE Healthcare Life Sciences, Logan, UT, USA), 1% penicillin-streptomycin (26253-84; NACALAI TESQUE, Kyoto, Kyoto, Japan), then incubated (95% air, 5% CO₂) at 37°C for 1 h. After cell culture, RNA extraction was performed using PureLink RNA Mini Kit (12183020; Thermo Fisher Scientific, Waltham, MA, USA). For RT-PCR, the extracted RNAs were reverse transcribed using the protocol supplied with ReverTra Ace qPCR RT Master Mix (FSQ-201; TOYOBO, Osaka, Osaka, Japan). StepOne Plus Real-time PCR System (Thermo Fisher Scientific, Waltham, MA, USA) was used to amplify and quantify levels of target gene cDNA. Quantitative PCR (q-PCR) was conducted using SsoAdvanced Universal SYBR Green Supermix (172-5271; BioRad Laboratories, Hercules, CA, United States) and specific primers for q-PCR. The sequences of primers used in this study are listed in **Supplementary Table 1**. Reactions were run in triplicate. The expression of each gene was normalized to the geometric mean of β -actin as a housekeeping gene and analyzed using the $\Delta\Delta$ CT method. Statistical analysis was performed using the GraphPad Prism7 (GraphPad Software). A two-tailed unpaired Student's *t*-test was applied to the q-PCR data. *P*-value < 0.05 was defined as the threshold.

Primary Cortical Neuron Culture of Mice

Cortical neurons were prepared from C57BL/6 mice on E16–17. Briefly, the mouse cerebral cortex was digested with 0.25

% trypsin and DNase for 15 min. Cells were passed through a 100 m nylon mesh. The resultant cell suspension was diluted with DMEM/F12 (Thermo Fisher Scientific, Waltham, MA, USA) supplemented with 10% fetal bovine serum (HyClone, SH30396.03, GE Healthcare Life Sciences, Logan, UT, USA) and 1% penicillin-streptomycin (26253-84; NACALAI TESQUE, Kyoto, Kyoto, Japan). Subsequently, the cells were plated on poly-D-lysine coated dishes and maintained at 37°C in 5% CO₂. The culture medium was replaced with a serum-free DMEM/F12 supplemented with B27 (Thermo Fisher Scientific, Waltham, MA, USA) 24 h after plating.

Immunocytochemistry of Primary Murine Cortical Neuron Culture

Cultured cortical neurons were fixed with 4% PFA for 1 h at room temperature and incubated with blocking solution containing 1% BSA and 0.1% Triton X-100 in PBS for 1 h. Primary antibodies, anti-TUJ1 (1:1000, 801201; BioLegend, San Diego, CA, USA) was applied overnight at 4°C. Fluorescent dye Alexa Fluor 488-conjugated anti-mouse IgG (715-545-151; Jackson ImmunoResearch, West Grove, PA, USA) was used as the secondary antibody.

Oxygen-Glucose Deprivation/Reoxygenation of Primary Cortical Neuron and Quantitative Polymerase Chain Reaction

The cultured cortical neurons were plated in DMEM without glucose (09891-25; NACALAI TESQUE, Kyoto, Kyoto, Japan), and 1% penicillin-streptomycin (26253-84; NACALAI TESQUE, Kyoto, Kyoto, Japan). Subsequently, the organoids were cultured in a hypoxic incubator (94% N₂, 5% CO₂, 1% O₂) at 37°C for 1 h. For reoxygenation, the medium was changed to Primary Neuron Basal Medium, then incubated (95% air, 5% CO₂) at 37°C for 1 h. After cell culture, RNA extraction was performed using PureLink RNA Mini Kit (12183020; Thermo Fisher Scientific, Waltham, MA, USA). For RT-PCR, the extracted RNAs were reverse transcribed using the protocol supplied with ReverTra Ace qPCR RT Master Mix (FSQ-201; TOYOBO, Osaka, Japan). StepOne Plus Real-time PCR System (Thermo Fisher Scientific, Waltham, MA, USA) was used to amplify and quantify levels of target gene cDNA. Quantitative PCR (q-PCR) was conducted using SsoAdvanced Universal SYBR Green Supermix (172-5271; BioRad Laboratories, Hercules, CA, United States) and specific primers for q-PCR. Primers used in this study are listed in **Supplementary Table 1**.

Cell culture and hypoxic condition were performed three times, and reactions were run in triplicate. The expression of each gene was normalized to the geometric mean of β -actin as a housekeeping gene and analyzed using the $\Delta\Delta CT$ method. Averaged relative quantification (RQ) was calculated from the average of three RQ values per three samples, every q-PCR. Therefore, one q-PCR demonstrated two averaged RQ values (Ctrl vs. OGD/R), and finally the data from three q-PCR demonstrated six averaged RQ values: three averaged RQ values of controlled samples vs. three averaged RQ after OGD/R.

Statistical analysis was performed using the GraphPad Prism7 (GraphPad Software). A two-tailed unpaired Student's *t*-test was applied to the q-PCR data. *P*-value < 0.05 was defined as the threshold.

RESULTS

Transcriptome Analysis of Human Brain Ischemic Stroke Model in a Dish

We used six cerebral organoids from one batch and treated three organoids with OGD/R, which is a well-established method of mimicking the pathological processes of ischemia (Hossmann, 1998), to generate a model of cerebral ischemia/reperfusion *in vitro*, and three for normoxic condition. We first cultured the human cerebral organoids for 42 days. Subsequently, these organoids were placed under OGD condition for 1 h and reoxygenation for 1 h. After OGD/R treatment or normoxic condition, RNAs were extracted from each human cerebral organoid prior to RNA isolation and RNA sequencing, of which samples were from every organoid sample, whereupon gene ontology analysis was performed (**Figure 1A**). Immunohistochemical staining of neuronal cells' marker (TUJ1) and DAPI showed the existence of neuronal cells in our organoids model (**Figure 1B**). Significant DEGs are colored in red (**Figure 1C**). Using the threshold of $p < 0.05$ and $|\log FC| > 0.1$, a total of 52 DEGs were determined between intact cerebral organoids and cerebral organoids under OGD/R, including 14 upregulated and 38 downregulated genes (**Table 1**). When false discovery rate (FDR) adjusted p -value ≤ 0.05 was used as a threshold, 15 genes of *AFP*, *TTR*, *APOA2*, *ALB*, *APOA1*, *RNA28SN4*, *APOC3*, *FTL*, *AHSG*, *FGG*, *FABP1*, *MIR3615*, *FGB*, *RNA45SN4*, and *FGA* were detected, and all genes were found to be downregulated (**Table 1**). The top five significant downregulated genes were *AFP*, *TTR*, *APOA2*, *ALB*, and *APOA1*, and upregulated genes were *RN7SL2*, *YWHAE*, *PTN*, *NNAT*, *RN7SL1*, *POSTN*, *DNAJB1*, *MIR6132*, *LOC105379506*, and *PEA15* (**Table 1**). In the brain, *YWHAE* is involved in directing the movement of nerve cells by binding to other proteins (Toyo-oka et al., 2003). Pleiotrophin (*PTN*), which is mainly expressed in the cerebral cortex (Kido et al., 2014; Shen et al., 2017), plays important roles in cell growth and survival, cell migration, and the expression of inflammatory cytokines (Shen et al., 2017), and *POSTN* leads to decreased apoptosis during hypoxia (Aukkarasongsup et al., 2013). These results indicate that upregulated genes might be associated with neuroprotection.

Co-expression Network Construction

To further investigate pathways involved in ischemic response of human brain, several network analyses were applied. Gene ontological (GO) analysis in the biological process category showed that OGD/R on human cerebral organoids induced lipid metabolism and blood coagulation (**Table 2**). The pathway-based analysis, KEGG pathway, further highlighted the vitamin digestion and absorption, fat digestion and absorption, peroxisome proliferator-activated receptor (PPAR) signaling pathway, and complement and coagulation cascades (**Table 3**). Using the STRING online database, 52 DEGs

TABLE 2 | Go term analysis derived from biological process of human cerebral organoids after OGD/R (FDR < 0.05).

Term	Count	P-value	FDR
Retinoid metabolic process	11	5.91E-17	1.55E-13
Platelet degranulation	9	5.07E-11	7.27E-08
Lipoprotein metabolic process	7	1.96E-10	2.81E-07
Cholesterol efflux	6	2.02E-09	2.89E-06
Lipoprotein biosynthetic process	5	2.49E-09	3.58E-06
Phospholipid efflux	5	1.97E-08	2.82E-05
High-density lipoprotein particle remodeling	5	2.68E-08	3.84E-05
Reverse cholesterol transport	5	5.97E-08	8.56E-05
Triglyceride catabolic process	5	2.44E-07	3.50E-04
Cholesterol homeostasis	6	2.72E-07	3.90E-04
High-density lipoprotein particle assembly	4	5.47E-07	7.85E-04
Positive regulation of cholesterol esterification	4	8.20E-07	0.001176
Protein polymerization	4	2.77E-06	0.003979
Negative regulation of very-low-density lipoprotein particle remodeling	3	1.42E-05	0.020297
Cholesterol metabolic process	5	1.47E-05	0.021062
Lipid transport	5	2.28E-05	0.032765
Triglyceride homeostasis	4	2.47E-05	0.035457
Blood coagulation, fibrin clot formation	3	2.83E-05	0.040534

were filtered by the PPI network of DEGs including nodes and edges with parameters of minimum required interaction score >0.4 (medium confidence) (Figure 2). These analyses revealed potential pathways involved in cellular response to ischemic stroke.

AHSG, TTR, and FGG Are Downregulated After OGD/R in the Human Cerebral Organoids

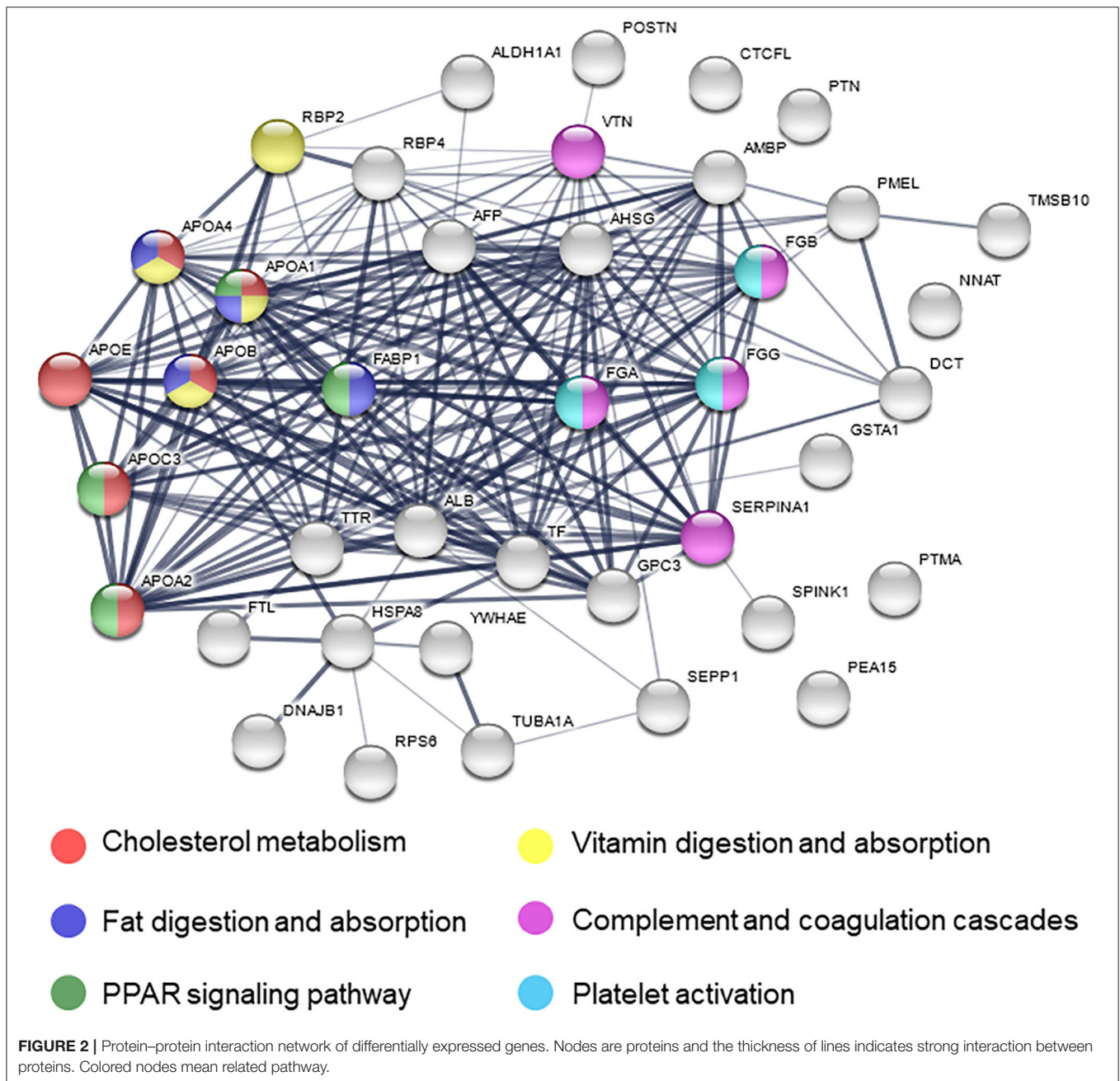
Next, we searched for important genes involved in neurological diseases. Among the affected genes after OGD/R in human cerebral organoids, transthyretin (*TTR*), alpha-2-HS-glycoprotein (*AHSG*), and fibrinogen gamma chain (*FGG*) were found to be related to neurological disease. *AHSG* is associated with alopecia-mental retardation syndrome 1 (Reza Sailani et al., 2017), patients of familial amyloid polyneuropathy (*FAP*) carrying *TTR* Met30 mutation (Tanaka et al., 1994), and fibrinogen gamma chain (*FGG*) appear to be protected after ischemic stroke (Cheung et al., 2008). By quantitative PCR (q-PCR), we confirmed downregulation of these three genes; *TTR*, *AHSG*, and *FGG* were significantly downregulated (Figure 3A). Our results suggest that these three genes have potential to contribute to pathogenesis of ischemic stroke in the human brain.

To find the genes that play more important roles in the brain, we then verified these three genes with gene expression

data of normal human tissues obtained from GTEx database. Though a vast majority of *AHSG* is secreted by the liver in adults (Figure 3B), *AHSG* is synthesized by various tissues at fetal stage (Stefan et al., 2006; Dabrowska et al., 2015). We demonstrated *AHSG* was downregulated after OGD/R in the human cerebral organoids (Figure 3A). Therefore, to validate *AHSG* expression after OGD/R in non-neural cells, human hepatocellular carcinoma (HepG2), human fibroblasts (hTERT-BJ), and human glioblastoma (U251MG), and murine microglia (BV2 cells) as neural cells were cultured and treated under OGD/R. *Ahsg* or *AHSG* expression of murine microglia, fibroblasts, and glioblastoma was unaltered after OGD/R (Figure 3C). *TTR* and *FGG* were not detected in BV2 cells and *TTR* was not detected in hTERT-BJ (Figure 3C). These results suggest that downregulated *AHSG* of human cerebral organoids might be specific to human fetal brain or human cerebral organoids. *AHSG* expression of hepatocellular carcinoma showed downward trend (1.43 fold; $P = 0.09$) after OGD/R (Figure 3C). This finding might indicate the existence of a cell type with similar gene expression to that of hepatic cells in human cerebral organoids.

Expression of *FTL* in Human Cerebral Organoids, Murine Cells, and Non-neural Cells

Ferritin light chain (*FTL*) is gene responsible for neurodegeneration with brain iron accumulation (Muhoberac and Vidal, 2019), and *FTL* was found to be abundantly expressed in the brain (Figure 4A). Although *FTL* was significantly downregulated after OGD/R by using RNA sequencing (Table 1), q-PCR analysis indicated a down-regulated trend of *FTL* (3.40 fold; $P = 0.18$) and no change to the ferritin heavy chain (*FTH*) in the cerebral organoids after OGD/R (Figure 4B). Immunohistochemical staining of neuronal cells' marker (TUJ1) showed the existence of neuronal cells in primary cultured cerebral cortical neurons of mice (Figure 4C). To examine the expression level of *FTL* in mice, the expression level of *Ftl* was tested and unaltered, using primary cultured murine cortical neurons and murine microglia (BV2 cells) treated with OGD/R (Figure 4D). *FTL* expression of OGD/R in non-neural cells, hepatocellular carcinoma (HepG2), telomerase reverse transcriptase immortalized fibroblasts (hTERT-BJ), and glioblastoma (U251MG), were 2D cultured and challenged by OGD/R. While the expression level of *FTL* was unaltered in hTERT-BJ and U251MG, it was downregulated by OGD/R treatment in HepG2 (Figure 4D). Additionally, to analyze the influence of different hypoxic conditions in non-neural cells (hTERT-BJ and U251MG), hTERT-BJ and U251MG cells were 2D cultured and treated by mild hypoxia (i.e., approximately 10% O₂ for 24 h). The expression level of *FTL* was upregulated by mild hypoxia treatment in both cell lines (Supplementary Figure 1B). In murine primary cultured neurons, fibroblast, and glioblastoma cells, *FTL* expression was not affected by OGD/R as severe hypoxia and might be a reaction specific to human cerebral organoids.



***PKM2* Is Upregulated by OGD/R in Human Cerebral Organoids and Mouse Cortical Neurons**

We validated some genes which could be indicators of hypoxia and ischemic markers for cerebral organoids and other cell types. Pyruvate kinase M2 (*PKM2*), which is associated with glycolytic pathway, converting glucose to lactate and generating ATP (Yang and Lu, 2015), is upregulated after OGD in murine dendritic cells (Jiang et al., 2018). Thus, we searched for important gene associated with hypoxia, and *PKM2* were significantly upregulated after OGD/R in the human cerebral organoids

(Figure 5A). Vascular endothelial growth factor (*VEGF*) was relatively upregulated (1.83 fold; $P = 0.15$) and hypoxia inducible factor 1A (*HIF1A*) were not clearly changed after OGD/R in human cerebral organoids (Figure 5A). BV2 cells, hTERT-BJ, U251MG, and HepG2 were cultured and treated under OGD/R. *Pkm2* and *PKM2* did not show significant change after OGD/R (Figure 5B). These results suggest that upregulation of *PKM2* of human cerebral organoids might be specific to humans. *VEGFA* upregulation was significantly verified in hTERT-BJ and U251MG, *Vegfa* was upregulated in BV2 cells, and *Vegfa* and *VEGFA* did not change in murine primary cultured neurons

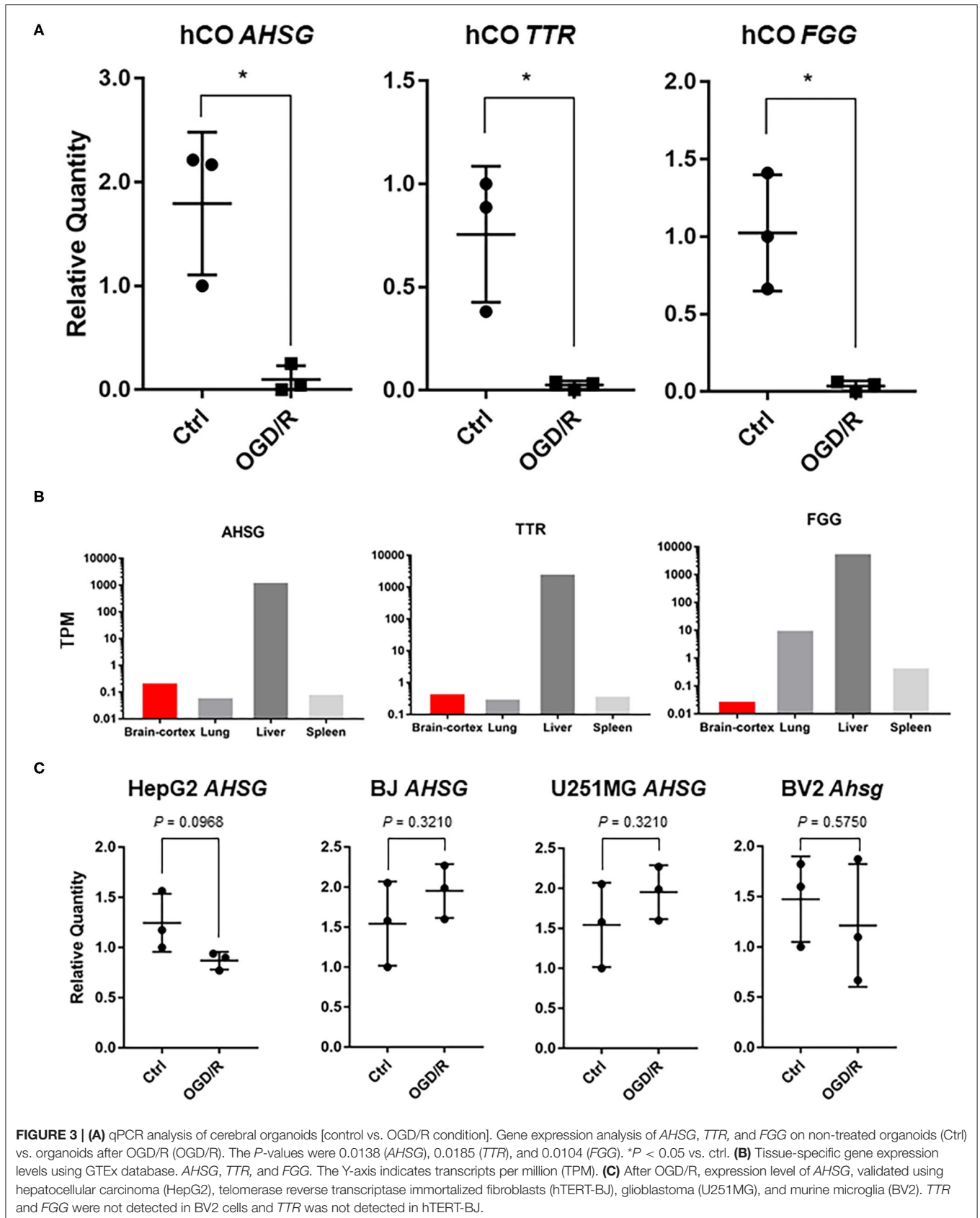
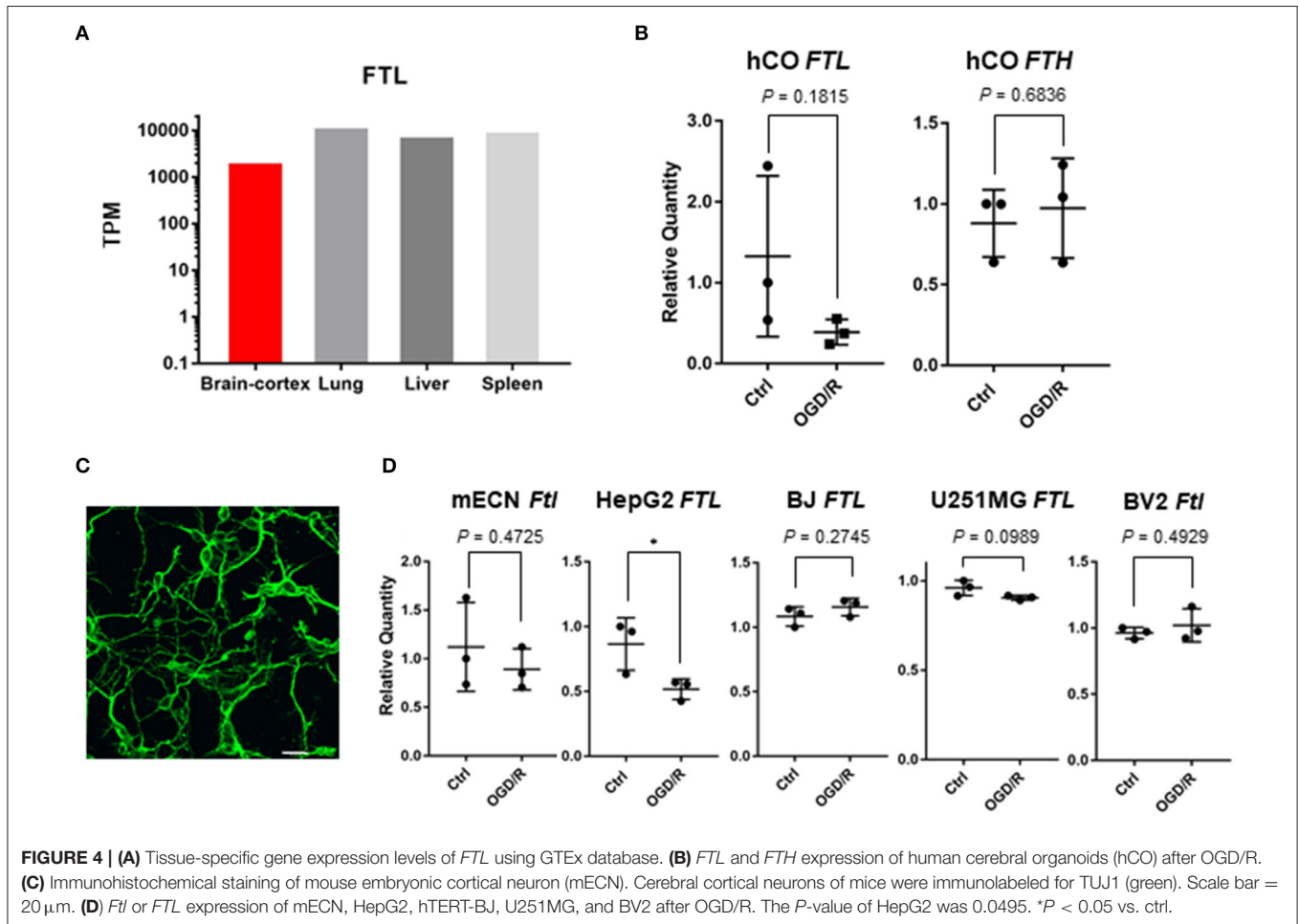


TABLE 3 | KEGG pathway of differentially expressed genes.

Term	Count	Genes	FDR	P-value
Vitamin digestion and absorption	4	APOA4, APOB, APOA1, RBP2	0.058366266	6.24E-05
Fat digestion and absorption	4	APOA4, APOB, APOA1, FABP1	0.332117918	3.56E-04
PPAR signaling pathway	4	APOA2, APOA1, APOC3, FABP1	1.618503332	0.0017426
Complement and coagulation cascades	4	FGG, FGA, FGB, SERPINA1	1.760575716	0.0018968
Platelet activation	3	FGG, FGA, FGB	54.24273463	0.0801693

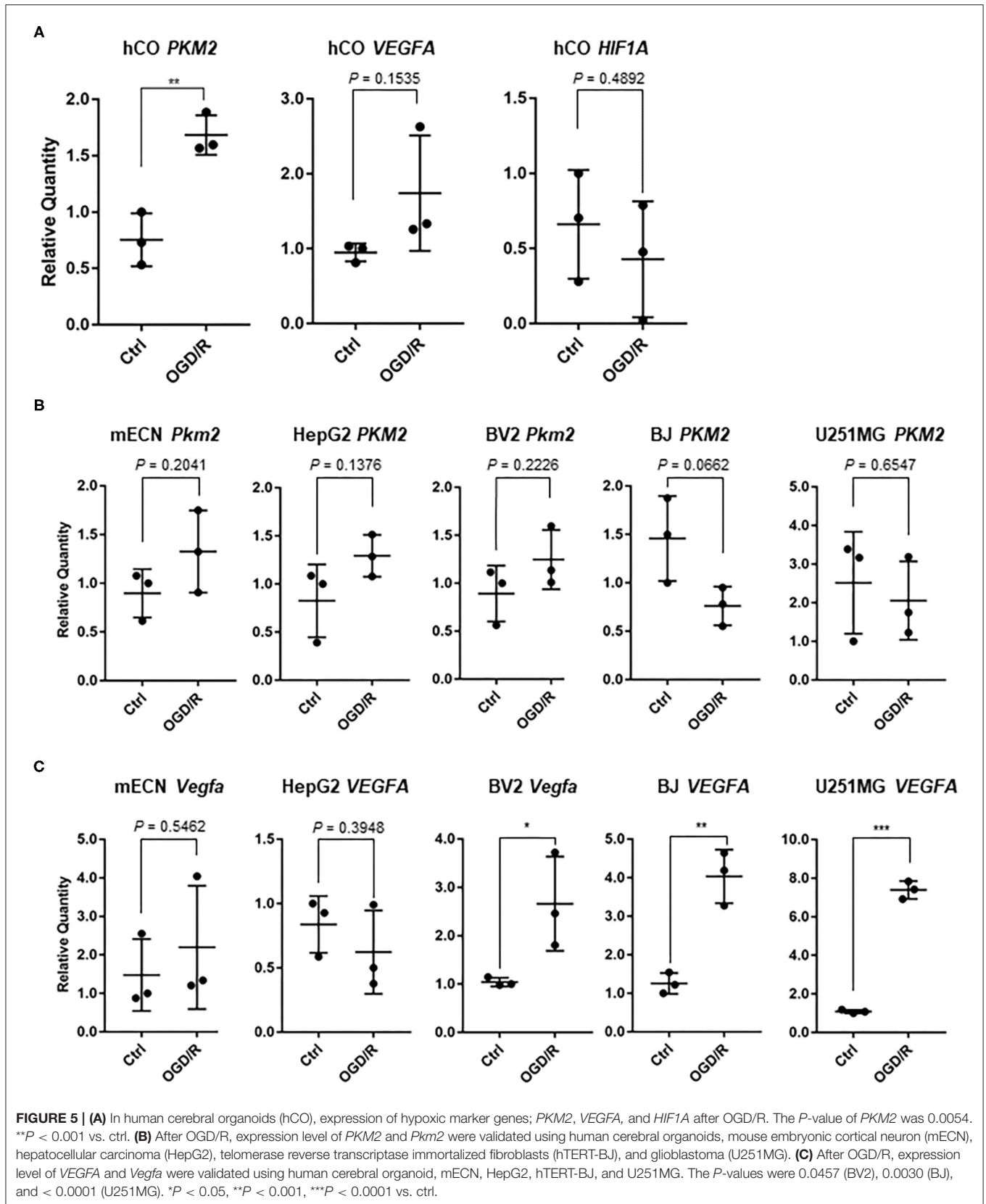


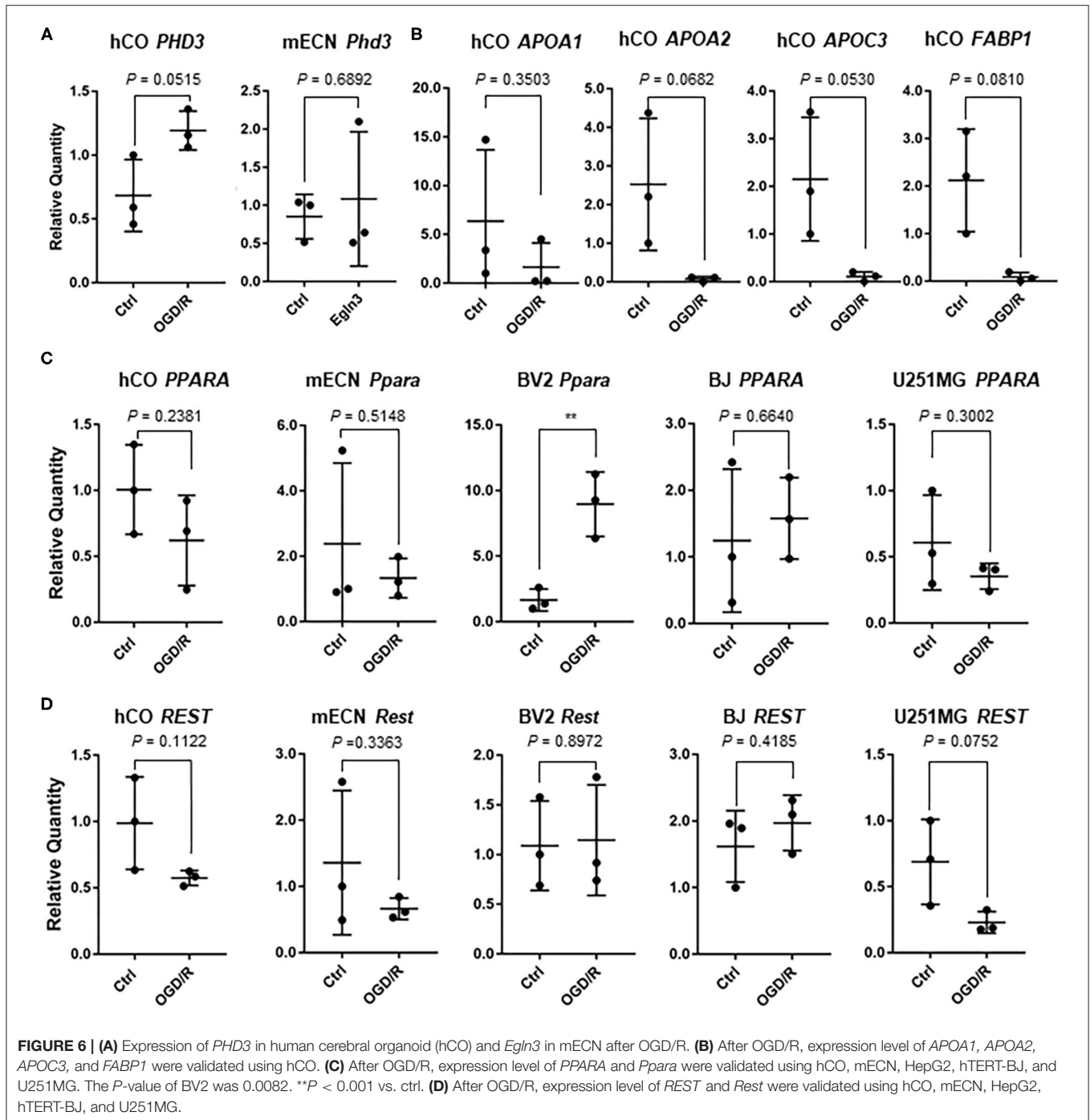
and HepG2 (Figure 5C). We found that the change of hypoxic marker genes independently showed various patterns in human cerebral organoids. We focused on some genes associated with transcriptional factors. Because prolyl hydroxylase 3 (PHD3, encoded by *EGLN3* gene) works as a co-activator of PKM2 and makes the connectivity of HIF1A and PKM2 strong (Luo et al., 2011), we validated expression of *PHD3/Egln3*. *PHD3* was relatively upregulated in organoids (1.74 fold; $P = 0.05$) (Figure 6A). According to pathway analysis of PPAR, we validated relatively downregulated apolipoprotein A1 (*APOA1*) (3.86 fold; $P = 0.35$), apolipoprotein A2 (*APOA2*) (33.28 fold; $P = 0.06$), apolipoprotein C3 (*APOC3*) (20.12 fold; $P = 0.05$), and fatty acid binding protein 1 (*FABP1*) (25.20 fold; $P = 0.08$) (Figure 6B). The expression level of *PPARA* as a nuclear

transcription factor was upregulated in BV2 cells and was not altered in other cell types (Figure 6C). Because the RE1-silencing transcription factor (*REST*) as another nuclear transcription factor works against the oxidative stress of aging brain and Alzheimer's Disease using immunostaining of human brain (Lu et al., 2014), we tested the expression level of *REST* and it was not clearly changed (Figure 6D).

DISCUSSION

In vivo models reflect many factors including central nervous system, vascular system, and immune systems, and the interaction and physiological systems make interpretations of the





results complex. On the contrary, *in vitro* 2D models consist of homotypic cell populations without cellular diversity and are unlikely to represent tissue architecture of actual tissues. Therefore, development and application of *in vitro* 3D model organoids are required to interpret the actual organ systems and cellular reactions. Additionally, *in vitro* maturation of human iPSC-derived 3D organoids could be a useful model for studying the pathophysiology of disease. Some genes of 3D cultured chondrocytes are highly increased and other genes are decreased

compared with 2D models (Caron et al., 2012), and kidney organoids are more sensitive to nephrotoxicity than 2D cultured cell lines (Astashkina et al., 2012). Although human cerebral organoids lack fully matured neuronal tissue, our model still provides a biologically plausible means to study ischemic injury response in the human brain tissue. By using human cerebral organoids combined with series of transcriptome analysis, we revealed that *TTR*, *AHSG*, and *FGG* were downregulated after OGD/R. Although we were able to detect a downregulation of

FTL in human cerebral organoids after OGD/R by using RNA-seq, we found no significant change in q-PCR. Simultaneously we validated unaltered *FTL* in non-neural cells (fibroblasts and glioblastoma), murine microglia, and primary cultured murine cortical neurons after OGD/R. A larger sample size of cerebral organoids is preferable for validating *FTL* expression level because there are differences in maturity among individual organoids. Although *FTL* was more expressed than *AHSG*, *TTR*, and *FGG* using gene expression data for normal human tissues (**Figures 3B, 4A**), it remains debatable whether iron itself and iron accumulation were beneficial or harmful after experimental stroke. Some groups have shown that brain damage after ischemia is correlated with overloaded iron (Castellanos et al., 2002; Mehta et al., 2004), while others suggest that iron storage is not evil (Christensen et al., 2002; Millerot et al., 2005). Therefore, further investigations are required to clarify the role of iron and iron storage after ischemic stroke.

We revealed that *FTL*, *TTR*, *AHSG*, and *FGG* are downregulated after OGD/R, but the distribution of *FTL*, *TTR*, *AHSG*, and *FGG* in human tissue is independent (**Figures 3B, 4A**). While *FTL*, *TTR*, *AHSG*, and *FGG* were abundantly expressed in liver, *TTR*, *AHSG*, and *FGG* were not sufficient in brain (**Figures 3B, 4A**). To validate the reaction of hepatocytes, we used HepG2 cells and *FTL* and *AHSG* tended to downregulate after OGD/R (**Figures 3C, 4D**). It could be possible that hepatocytes or hepatocyte-like cells co-exist in the human cerebral organoids. Although cell types of the human cerebral organoids are derived from ectodermal origin (Quadrato et al., 2017), hepatic cells are derived from endoderm origin. There might be co-existing hepatic cells or hepatocyte-like cells in the human cerebral organoids we used in this study, and this might be potential limitations of the current study.

We revealed the expression level of *PKM2* of the human cerebral organoids after OGD/R was predominantly elevated. On the contrary the expression level of *PKM2* of other cells after OGD/R was not evidently changed. *Pkm2*, both mRNA and protein, is upregulated after OGD in murine dendritic cells, which are immune-modulatory cells that do not exist in our human cerebral organoids (Jiang et al., 2018). These results suggest that the upregulation of *PKM2* might be useful as a hypoxic marker in human cerebral organoids, while an expression of *PKM2* might be controversial in other cell types. Although *PKM2* plays protective role in acute phase of focal ischemic stroke model of mice (Chen et al., 2018), loss of *Pkm2* using *Pkm2* knockout mice also protects ischemic tissues by maintaining mitochondrial biogenesis (Hauck et al., 2020). Thus, the role of *PKM2* upon OGD/R insults is still controversial. *PKM2* is a target gene of HIF-1 α , regulates gene expression of proteins associated with the glycolytic pathway and can accelerate metabolic reprogramming (Luo et al., 2011). Furthermore, *PHD3/Egln3* induced by hypoxia works as a co-activator of *PKM2* by HIF pathway (Pescador et al., 2005). *PHD3/Egln3* is relatively upregulated after OGD/R. This might accelerate metabolic switch and lead to decreased high-density lipoproteins (HDLs) including *APOA1*, *APOA2*, and *APOC3*, all of which showed a trend of downregulation upon OGD/R

(**Figure 6B**). Therefore, *PKM2* may act synergistically with *PHD3/Hif-1 α* in our OGD/R model. On the other hand, although some genes about fatty acid were relatively downregulated (**Figure 6B**), *PPARA* downregulation was validated only in murine microglia (**Figure 6C**). The reason why *PPARA* was unchanged in cerebral organoids might be due to a lack of microglia derived from mesoderm. Novel system of cerebral organoids including microglia will resolve this limitation. *REST* is a transcriptional factor as a silencer, concerning neurogenesis, neuronal differentiation, and growth (Paquette et al., 2000). We validated relatively downregulated *REST* in cerebral organoids, not murine primary cultured neurons (**Figure 6D**). Because some genes about neuronal movement, growth, and survival were upregulated after OGD/R using RNA-seq data set, *REST* downregulation might lead to neurogenesis and neuronal differentiation. These results could be specific for 3D embryonic culture system. *PKM2* is inhibited by *PPAR γ* in two breast cancer cell lines, and this inhibition might decrease ATP levels and avoid apoptosis (Shashni et al., 2013). We showed *PPAR* signaling pathway is associated (**Figure 2**) and *PKM2* was upregulated after OGD/R in human cerebral organoids (**Figure 5A**). This could suggest that *PPAR γ* is downregulated and *PKM2* is upregulated subsequently after ischemia. The *PPAR γ* agonist conducts neuroprotection against focal ischemia in the rat brain (Zhao et al., 2005). Dual *PPAR α/γ* agonist improves stroke outcome after transient cerebral ischemia in mice (Boujon et al., 2019). Therefore, therapeutic agents related lipid metabolism, including *PPAR* agonist, may be effective for ischemia.

Our study did not clarify either the change of common hypoxic marker genes (*VEGF* and *HIF1A*) of human cerebral organoids occurs after OGD/R (**Figures 5A,C**) or a change in other hypoxic marker genes (*LDHA*, *CA9*, and *PGK1*) (**Supplementary Figure 1C**). Lacking vascular system, brain organoids necrotize in their core as they grow and exist around the core healthy tissues *in vitro* (Lancaster, 2018). To resolve the problem of central core necrosis of brain organoids, they are transplanted into the mouse brain as vascularized model of brain organoids *in vivo* (Mansour et al., 2018). *In vitro* organotypic slice culture improved long-term survival (Giandomenico et al., 2021), and air-liquid interface culture for cerebral organoids improved survival, axon outgrowth, and decreased apoptosis rate (Giandomenico et al., 2019). It might be the reason why *VEGFA* and *HIF1A* did not significantly change, and the lack of vascular system was one of the limitation of cerebral organoids. Although *VEGF* and *HIF1A* were not markedly upregulated, we validated upregulated *HSPA8*, stress-induced protein: heat-shock cognate protein 70 (*HSC70*) coding gene, using RNA-seq (**Table 1**). Because *HSC70* assembles after cerebral ischemia of rats (Hu et al., 1998) and *HSC70* involves diverse proteostasis mechanisms including chaperone mediated autophagy which contributes to oxidative stress response (Kiffin et al., 2004; Loeffler et al., 2016), upregulated *HSPA8* coding *HSC70* indicated the oxidative stress of our model was existing.

There are a number of groups trying to apply organoid system to study isolated organ model in a dish. For example, James Hudson and colleagues showed that mild-hypoxia and/or metabolic changes are critical environmental triggers

for maturation of cardiac cells using human cardiac organoids (Mills et al., 2019). In their experiments, they treated the human cardiac organoids by changing the serum free media, lowering glucose concentration, and increasing the concentration of fatty acid. Palmitate was used as a fatty acid substrate, as it is one of the most abundant fatty acids circulating during the neonatal period (Bougnères et al., 1982). Importantly, Hesham Sadek and colleagues discovered mild-hypoxia to be a stimulus for the metabolic switch from carbohydrates to fatty acids in a neonatal mouse cardiac tissue (Puente et al., 2014) and adult mouse cardiac tissue (Nakada et al., 2017), and therefore human cardiac organoids could model the postnatal switch in metabolic substrates from carbohydrates to fatty acids. In our experiment, we removed glucose and oxygen without substituting fatty acid. Thus, the human brain organoids do not get substrates even if the gene expression may alter metabolic switch from carbohydrates to fatty acids. The difference of *FTL* expression between mild-hypoxia and severe-hypoxia **Figure 4D**, **Supplementary Figure 1B** might suggest mild-hypoxia tends to metabolize fatty acid, compared with severe-hypoxia. Taken together, our experimental condition is not comparable to environmental changes that induce postnatal metabolic shift; instead, it mimics ischemic tissue. More detailed time course about hypoxia will be needed for further investigation in the future. It is possible that neural cells in the brain and cardiac muscle cells in the heart may respond differentially to severe hypoxia. Therefore, in order to adapt their findings from the cardiac organoids (Mills et al., 2017) to our brain organoids, neural cells would need to have similar capability to respond to same environmental stimuli. Further investigations are required to understand how neural and non-neural cells in the brain respond to pathogenic severe hypoxia.

Our goal here is to extract the direct effects on neural tissues out of spatio-temporally complex system organized by various cell types. Our cerebral organoids are free from the effect of blood vessels and blood-derived inflammatory cells invading through blood vessels. Therefore, our experimental model enabled us to evaluate the direct effect of deprivation of both oxygen and glucose followed by reoxygenation on brain tissue. Although we are aware of the limitations of applying the human cerebral organoid as a model for human ischemic stroke, there are expectations for the potential development and advancement for further applications of our model.

DATA AVAILABILITY STATEMENT

The datasets presented in this study can be found in online repositories. The names of the repository/repositories and accession number(s) can be found below: <https://www.ddbj.nig.ac.jp/>, DRA010225.

ETHICS STATEMENT

The animal study was reviewed and approved by Animal Care Committee of Nara Medical University.

AUTHOR CONTRIBUTIONS

NIw, TM, KSu, and EM designed the study. NIw, TM, NIg, KK, NM, YMS, TS, SKo, TT, MN, and RN conducted the research. NIw, TM, NIg, KK, YMS, MM, NE, TK, TI, KSa, HK, YS, WK, AW, YN, EM, and KSu analyzed the data. NIw, TM, TT, KSu, and EM wrote the paper. All authors contributed to manuscript revision and read and approved the submitted version.

FUNDING

This work was supported by grants from JSPS KAKENHI (JP17H07031, JP20H03199 to EM, JP19K16925 to TM, JP19K07978 to TK), AMED Brain/MINDS Beyond (JP20dm0307032 to EM), AMED The Program for Technological Innovation of Regenerative Medicine (JP20bm0704039 to TM), AMED Osaka University Seeds (A) to TM, Takeda Science Foundation to EM and TM, Kanzawa Medical Research Foundation to EM, Uehara Memorial Foundation to EM, Nakatomi Foundation to EM, Konica Minolta Science and Technology Foundation to EM, Naito Foundation to EM, MSD Life Science Foundation to EM, Mochida Memorial Foundation for Medical and Pharmaceutical Research to EM, SENSHIN Medical Research Foundation to EM, Terumo Foundation for Life Sciences and Arts to EM, Nara Kidney Disease Research Foundation to EM, Novartis Research Grants to EM and KSu, Sumitomo Dainippon Pharma Research Grant to TM, Nara Medical University Grant-in-Aid for Collaborative Research Projects to KSu, Nara Medical University Grant-in-Aid for Young Scientists to TM, and by unrestricted funds provided to EM from Dr. Taichi Noda (KTX Corp., Aichi, Japan) and Dr. Yasuhiro Horii (Koseikai, Nara, Japan). The authors declare that this study received funding from parties mentioned above. The funders were not involved in the study design, collection, analysis, interpretation of data, the writing of this article or decision to submit the article for publication.

ACKNOWLEDGMENTS

The authors thank Keren-Happuch E. Fan Fen for her critical reading of the manuscript. hTERT-BJ were kindly gifted by Keiji Suzuki (Department of Radiation Medical Sciences, Atomic Bomb Disease Institute, Nagasaki University, Nagasaki, Japan).

This manuscript has been released as a Pre-Print at bioRxiv (Iwasa et al., 2020).

SUPPLEMENTARY MATERIAL

The Supplementary Material for this article can be found online at: <https://www.frontiersin.org/articles/10.3389/fncel.2021.605030/full#supplementary-material>

Supplementary Figure 1 | (A) Immunohistochemical staining of mouse embryonic cortical neuron (mECN). Cerebral cortical neurons of mice were immunolabeled for TUJ1 (green). Scale bar = 100 μ m. **(B)** Expression level of *FtI* and *FTL* under mild hypoxia (i.e., O₂ 10% for 24 h). **(C)** In hCO, expression of other hypoxic marker genes; *LDHA*, *CA9*, and *PGK1* after OGD/R.

Supplementary Table 1 | Primer pairs for qPCRs used in this study.

REFERENCES

- Astashkina, A. I., Mann, B. K., Prestwich, G. D., and Grainger, D. W. (2012). Comparing predictive drug nephrotoxicity biomarkers in kidney 3-D primary organoid culture and immortalized cell lines. *Biomaterials* 33, 4712–4721. doi: 10.1016/j.biomaterials.2012.03.001
- Aukkarasongsup, P., Haruyama, N., Matsumoto, T., Shiga, M., and Moriyama, K. (2013). Periostin inhibits hypoxia-induced apoptosis in human periodontal ligament cells via TGF-beta signaling. *Biochem. Biophys. Res. Commun.* 441, 126–132. doi: 10.1016/j.bbrc.2013.10.027
- Benjamin, E. J., Muntner, P., Alonso, A., Bittencourt, M. S., Callaway, C. W., Carson, A. P., et al. (2019). Heart disease and stroke statistics-2019 update: a report from the American heart association. *Circulation* 139, e56–e528. doi: 10.1161/cir.0000000000000659
- Bougnères, P. F., Karl, I. E., Hillman, L. S., and Bier, D. M. (1982). Lipid transport in the human newborn. Palmitate and glycerol turnover and the contribution of glycerol to neonatal hepatic glucose output. *J. Clin. Invest.* 70, 262–270. doi: 10.1172/jci110613
- Boujon, V., Uhlemann, R., Wegner, S., Wright, M. B., Laufs, U., Endres, M., et al. (2019). Dual PPAR α/γ agonist aeligitarz confers stroke protection in a model of mild focal brain ischemia in mice. *J. Mol. Med. (Berl)*. 97, 1127–1138. doi: 10.1007/s00109-019-01801-0
- Caron, M. M., Emans, P. J., Coolen, M. M., Voss, L., Surtel, D. A., Cremers, A., et al. (2012). Redifferentiation of dedifferentiated human articular chondrocytes: comparison of 2D and 3D cultures. *Osteoarthritis Cartilage* 20, 1170–1178. doi: 10.1016/j.joca.2012.06.016
- Castellanos, M., Puig, N., Carbonell, T., Castillo, J., Martinez, J., Rama, R., et al. (2002). Iron intake increases infarct volume after permanent middle cerebral artery occlusion in rats. *Brain Res.* 952, 1–6. doi: 10.1016/s0006-8993(02)03179-7
- Catanese, L., Tarsia, J., and Fisher, M. (2017). Acute ischemic stroke therapy overview. *Circ. Res.* 120, 541–558. doi: 10.1161/circresaha.116.309278
- Chen, D., Wei, L., Liu, Z. R., Yang, J. J., Gu, X., Wei, Z. Z., et al. (2018). Pyruvate kinase M2 increases angiogenesis, neurogenesis, and functional recovery mediated by upregulation of STAT3 and focal adhesion kinase activities after ischemic stroke in adult mice. *Neurotherapeutics* 15, 770–784. doi: 10.1007/s13311-018-0635-2
- Cheung, E. Y., Uitte de Willige, S., Vos, H. L., Leebeek, F. W., Dippel, D. W., Bertina, R. M., et al. (2008). Fibrinogen gamma' in ischemic stroke: a case-control study. *Stroke* 39, 1033–1035. doi: 10.1161/strokeaha.107.495499
- Christensen, H., Boysen, G., Johannesen, H. H., Christensen, E., and Bendtzen, K. (2002). Deteriorating ischaemic stroke. cytokines, soluble cytokine receptors, ferritin, systemic blood pressure, body temperature, blood glucose, diabetes, stroke severity, and CT infarction-volume as predictors of deteriorating ischaemic stroke. *J. Neurol. Sci.* 201, 1–7. doi: 10.1016/s0022-510x(02)00160-0
- Clevers, H. (2016). Modeling development and disease with organoids. *Cell* 165, 1586–1597. doi: 10.1016/j.cell.2016.05.082
- Dabrowska, A. M., Tarach, J. S., Wojtyasiak-Duma, B., and Duma, D. (2015). Fetuin-A (AHSG) and its usefulness in clinical practice. Review of the literature. *Biomed. Pap. Med. Fac. Univ. Palacky. Olomouc. Czech. Repub.* 159, 352–359. doi: 10.5507/bp.2015.018
- Dorado, L., Millan, M., and Davalos, A. (2014). Reperfusion therapies for acute ischemic stroke: an update. *Curr. Cardiol. Rev.* 10, 327–335. doi: 10.2174/1573403x10666140320144637
- Fisher, M., and Bastan, B. (2012). Identifying and utilizing the ischemic penumbra. *Neurology* 79(13 Suppl 1), S79–S85. doi: 10.1212/WNL.0b013e3182695814
- Giandomenico, S. L., Mierau, S. B., Gibbons, G. M., Wenger, L. M. D., Masullo, L., Sit, T., et al. (2019). Cerebral organoids at the air-liquid interface generate diverse nerve tracts with functional output. *Nat. Neurosci.* 22, 669–679. doi: 10.1038/s41593-019-0350-2
- Giandomenico, S. L., Sutcliffe, M., and Lancaster, M. A. (2021). Generation and long-term culture of advanced cerebral organoids for studying later stages of neural development. *Nat. Protoc.* 16, 579–602. doi: 10.1038/s41596-020-00433-w
- Hauck, L., Dadson, K., Chauhan, S., Grothe, D., and Billia, F. (2020). Inhibiting the Pkm2/b-catenin axis drives *in vivo* replication of adult cardiomyocytes following experimental MI. *Cell Death Differ.* 28, 1398–1417. doi: 10.1038/s41418-020-00669-9
- Hossmann, K. A. (1998). Experimental models for the investigation of brain ischemia. *Cardiovasc. Res.* 39, 106–120. doi: 10.1016/s0008-6363(98)00075-3
- Hu, B. R., Park, M., Martone, M. E., Fischer, W. H., Ellisman, M. H., and Zivin, J. A. (1998). Assembly of proteins to postsynaptic densities after transient cerebral ischemia. *J. Neurosci.* 18, 625–633. doi: 10.1523/jneurosci.18-02-00625.1998
- Iwasa, N., Matsui, T. K., Morikawa, N., Sakaguchi, Y. M., Shiota, T., Iguchi, N., et al. (2020). Oxygen-glucose deprivation and reoxygenation on human cerebral organoids alters expression related to lipid metabolism. *bioRxiv [Preprint]*. doi: 10.1101/2020.03.31.017335
- Jiang, H., Zhang, S., Song, T., Guan, X., Zhang, R., and Chen, X. (2018). Trichostatin A protects dendritic cells against oxygen-glucose deprivation via the SRSF3/PKM2/glycolytic pathway. *Front. Pharmacol.* 9:612. doi: 10.3389/fphar.2018.00612
- Kido, M., Nakamura, Y., Nemoto, K., Takahashi, T., Aleksic, B., Furuichi, A., et al. (2014). The polymorphism of YWHAE, a gene encoding 14-3-3epsilon, and brain morphology in schizophrenia: a voxel-based morphometric study. *PLoS ONE* 9:e103571. doi: 10.1371/journal.pone.0103571
- Kiffin, R., Christian, C., Knecht, E., and Cuervo, A. M. (2004). Activation of chaperone-mediated autophagy during oxidative stress. *Mol. Biol. Cell* 15, 4829–4840. doi: 10.1091/mbc.e04-06-0477
- Knowland, D., Arac, A., Sekiguchi, K. J., Hsu, M., Lutz, S. E., Perrino, J., et al. (2014). Stepwise recruitment of transcellular and paracellular pathways underlies blood-brain barrier breakdown in stroke. *Neuron* 82, 603–617. doi: 10.1016/j.neuron.2014.03.003
- Lancaster, M. A. (2018). Brain organoids get vascularized. *Nat. Biotechnol.* 36, 407–408. doi: 10.1038/nbt.4133
- Lancaster, M. A., Renner, M., Martin, C. A., Wenzel, D., Bicknell, L. S., Hurler, M. E., et al. (2013). Cerebral organoids model human brain development and microcephaly. *Nature* 501, 373–379. doi: 10.1038/nature12517
- Loeffler, D. A., Klaver, A. C., Coffey, M. P., Aasly, J. O., and LeWitt, P. A. (2016). Age-related decrease in heat shock 70-kDa protein 8 in cerebrospinal fluid is associated with increased oxidative stress. *Front. Aging Neurosci.* 8:178. doi: 10.3389/fnagi.2016.00178
- Lu, T., Aron, L., Zullo, J., Pan, Y., Kim, H., Chen, Y., et al. (2014). REST and stress resistance in ageing and Alzheimer's disease. *Nature* 507, 448–454. doi: 10.1038/nature13163
- Luo, W., Hu, H., Chang, R., Zhong, J., Knabel, M., O'Meally, R., et al. (2011). Pyruvate kinase M2 is a PHD3-stimulated coactivator for hypoxia-inducible factor 1. *Cell* 145, 732–744. doi: 10.1016/j.cell.2011.03.054
- Mansour, A. A., Gonçalves, J. T., Bloyd, C. W., Li, H., Fernandes, S., Quang, D., et al. (2018). An *in vivo* model of functional and vascularized human brain organoids. *Nat. Biotechnol.* 36, 432–441. doi: 10.1038/nbt.4127
- Mehta, S. H., Webb, R. C., Ergul, A., Tawfik, A., and Dorrance, A. M. (2004). Neuroprotection by tempol in a model of iron-induced oxidative stress in acute ischemic stroke. *Am. J. Physiol. Regul. Integr. Comp. Physiol.* 286, R283–R288. doi: 10.1152/ajpregu.00446.2002
- Millerot, E., Prigent-Tessier, A. S., Bertrand, N. M., Faure, P. J., Mossiat, C. M., Giroud, M. E., et al. (2005). Serum ferritin in stroke: a marker of increased body iron stores or stroke severity? *J. Cereb. Blood Flow Metab.* 25, 1386–1393. doi: 10.1038/sj.jcbfm.9600140
- Mills, R. J., Parker, B. L., Quaife-Ryan, G. A., Voges, H. K., Needham, E. J., Bornot, A., et al. (2019). Drug screening in human PSC-cardiac organoids identifies pro-proliferative compounds acting via the mevalonate pathway. *Cell Stem Cell* 24, 895.e896–907.e896. doi: 10.1016/j.stem.2019.03.009
- Mills, R. J., Titmarsh, D. M., Koenig, X., Parker, B. L., Ryall, J. G., Quaife-Ryan, G. A., et al. (2017). Functional screening in human cardiac organoids reveals a metabolic mechanism for cardiomyocyte cell cycle arrest. *Proc. Natl. Acad. Sci. U.S.A.* 114, E8372–E8381. doi: 10.1073/pnas.1707316114
- Muhoberac, B. B., and Vidal, R. (2019). Iron, ferritin, hereditary ferritinopathy, and neurodegeneration. *Front. Neurosci.* 13:1195. doi: 10.3389/fnins.2019.01195
- Nakada, Y., Canseco, D. C., Thet, S., Abdilsalam, S., Asaithamby, A., Santos, C. X., et al. (2017). Hypoxia induces heart regeneration in adult mice. *Nature* 541, 222–227. doi: 10.1038/nature20173
- Paquette, A. J., Perez, S. E., and Anderson, D. J. (2000). Constitutive expression of the neuron-restrictive silencer factor (NRSF)/REST in differentiating neurons disrupts neuronal gene expression and causes axon pathfinding errors *in vivo*. *Proc. Natl. Acad. Sci. U.S.A.* 97, 12318–12323. doi: 10.1073/pnas.97.22.12318

- Pasca, A. M., Sloan, S. A., Clarke, L. E., Tian, Y., Makinson, C. D., Huber, N., et al. (2015). Functional cortical neurons and astrocytes from human pluripotent stem cells in 3D culture. *Nat. Methods* 12, 671–678. doi: 10.1038/nmeth.3415
- Pescador, N., Cuevas, Y., Naranjo, S., Alcaide, M., Villar, D., Landázuri, M. O., et al. (2005). Identification of a functional hypoxia-responsive element that regulates the expression of the egl nine homologue 3 (egln3/phd3) gene. *Biochem. J.* 390(Pt 1), 189–197. doi: 10.1042/bj20042121
- Puente, B. N., Kimura, W., Muralidhar, S. A., Moon, J., Amatruda, J. F., Phelps, K. L., et al. (2014). The oxygen-rich postnatal environment induces cardiomyocyte cell-cycle arrest through DNA damage response. *Cell* 157, 565–579. doi: 10.1016/j.cell.2014.03.032
- Quadrato, G., Nguyen, T., Macosko, E. Z., Sherwood, J. L., Min Yang, S., Berger, D. R., et al. (2017). Cell diversity and network dynamics in photosensitive human brain organoids. *Nature* 545, 48–53. doi: 10.1038/nature22047
- Reza Sailani, M., Jahanbani, F., Nasiri, J., Behnam, M., Salehi, M., Sedghi, M., et al. (2017). Association of AHSG with alopecia and mental retardation (APMR) syndrome. *Hum. Genet.* 136, 287–296. doi: 10.1007/s00439-016-1756-5
- Robinson, M. D., McCarthy, D. J., and Smyth, G. K. (2010). edgeR: a Bioconductor package for differential expression analysis of digital gene expression data. *Bioinformatics* 26, 139–140. doi: 10.1093/bioinformatics/btp616
- Shashni, B., Sakharkar, K. R., Nagasaki, Y., and Sakharkar, M. K. (2013). Glycolytic enzymes PGK1 and PKM2 as novel transcriptional targets of PPAR γ in breast cancer pathophysiology. *J. Drug Target* 21, 161–174. doi: 10.3109/1061186x.2012.736998
- Shen, D., Podolnikova, N. P., Yakubenko, V. P., Ardell, C. L., Balabiyev, A., Ugarova, T. P., et al. (2017). Pleiotrophin, a multifunctional cytokine and growth factor, induces leukocyte responses through the integrin Mac-1. *J. Biol. Chem.* 292, 18848–18861. doi: 10.1074/jbc.M116.773713
- Spescha, R. D., Shi, Y., Wegener, S., Keller, S., Weber, B., Wyss, M. M., et al. (2013). Deletion of the ageing gene p66(Shc) reduces early stroke size following ischaemia/reperfusion brain injury. *Eur. Heart J.* 34, 96–103. doi: 10.1093/eurheartj/ehs331
- Stefan, N., Hennige, A. M., Staiger, H., Machann, J., Schick, F., Kröber, S. M., et al. (2006). Alpha2-Heremans-Schmid glycoprotein/fetuin-A is associated with insulin resistance and fat accumulation in the liver in humans. *Diabetes Care* 29, 853–857. doi: 10.2337/diacare.29.04.06.dc05-1938
- Szklarczyk, D., Gable, A. L., Lyon, D., Junge, A., Wyder, S., Huerta-Cepas, J., et al. (2019). STRING v11: protein-protein association networks with increased coverage, supporting functional discovery in genome-wide experimental datasets. *Nucleic Acids Res.* 47, D607–D613. doi: 10.1093/nar/gky1131
- Tanaka, Y., Ando, Y., Kumamoto, T., Miyazaki, A., Nakamura, M., Nakayama, M., et al. (1994). Changed affinity of apolipoprotein AII to high density lipoprotein (HDL) in patients with familial amyloidotic polyneuropathy (FAP) type I. *Biochim. Biophys. Acta* 1225, 311–316. doi: 10.1016/0925-4439(94)0012-4
- Toyo-oka, K., Shionoya, A., Gambello, M. J., Cardoso, C., Leventer, R., Ward, H. L., et al. (2003). 14-3-3epsilon is important for neuronal migration by binding to NUDEL: a molecular explanation for Miller-Dieker syndrome. *Nat. Genet.* 34, 274–285. doi: 10.1038/ng1169
- Yang, W., and Lu, Z. (2015). Pyruvate kinase M2 at a glance. *J. Cell Sci.* 128, 1655–1660. doi: 10.1242/jcs.166629
- Zhao, Y., Patzer, A., Gohlke, P., Herdegen, T., and Culman, J. (2005). The intracerebral application of the PPARgamma-ligand pioglitazone confers neuroprotection against focal ischaemia in the rat brain. *Eur. J. Neurosci.* 22, 278–282. doi: 10.1111/j.1460-9568.2005.04200.x

Conflict of Interest: The authors declare that the research was conducted in the absence of any commercial or financial relationships that could be construed as a potential conflict of interest.

Copyright © 2021 Iwasa, Matsui, Iguchi, Kinugawa, Morikawa, Sakaguchi, Shiota, Kobashigawa, Nakanishi, Matsubayashi, Nagata, Kikuchi, Tanaka, Eura, Kiriyama, Izumi, Saito, Kataoka, Saito, Kimura, Wanaka, Nishimura, Mori and Sugie. This is an open-access article distributed under the terms of the Creative Commons Attribution License (CC BY). The use, distribution or reproduction in other forums is permitted, provided the original author(s) and the copyright owner(s) are credited and that the original publication in this journal is cited, in accordance with accepted academic practice. No use, distribution or reproduction is permitted which does not comply with these terms.